

Review

Graphene-Oxide Nano Composites for Chemical Sensor Applications

Surajit Kumar Hazra ¹ and Sukumar Basu ^{2,*}

¹ Department of Physics & Materials Science, Jaypee University of Information Technology, Solan District, 173234 Himachal Pradesh, India; surajithazra@yahoo.co.in

² Materials Science Center, Indian Institute of Technology (IIT), 721302 Kharagpur, India

* Correspondence: sukumarbasu@gmail.com; Tel.: +91-983-037-7105

Academic Editor: Vijay Kumar Thakur

Received: 26 February 2016; Accepted: 7 April 2016; Published: 12 April 2016

Abstract: Of late, graphene has occupied the attention of almost all researchers working globally in the area of materials science. Graphene nanocomposites are the latest additions to the wonder applications of graphene. One of the promising applications of the graphene-oxide nanocomposites is chemical sensing which is useful for monitoring the toxicity, inflammability, and explosive nature of chemicals. Well known binary oxides like ZnO, TiO₂, SnO₂, WO₃, and CuO when combined with graphene in the form of nanocomposites have excellent potential for detecting trace amounts of hazardous gases and chemicals. In this article the preparations, characterizations, and the chemical sensor applications of graphene-oxide nanocomposites are presented in detail.

Keywords: graphene; graphene oxides; binary metal oxides; nano composites; chemical sensors

1. Introduction

Chemical sensors have recently occupied a center stage in the area of research and development because of increasing environmental pollution, spread of life-threatening diseases, and terrorism throughout the world. Detection of trace amount of gases and chemicals using chemical sensors is the most modern technology to monitor and control the quality of air around the human inhabitant. Importance of innovative materials for the development of state-of-the-art chemical sensors for domestic and industrial applications is well recognized by the sensor community. Chemical sensors also have potential applications in the nuclear, space, and energy sectors. The repeatable and reliable sensing characteristics are mostly governed by the sensing material. Also, the optimum sensing temperature depends on the sensing material. Moreover, excellent electronic transport properties of the sensing material can improve the device characteristics like response, response time, and recovery time. The recent discovery of graphene has led to the revelation of promising material and sensing qualities [1]. Based on the reports so far, graphene is quite a suitable material for all types of chemical sensor applications because it has excellent structural, electrical, and chemical properties. The 2-dimensional (2D) nature of graphene increases its suitability for miniaturization of thin film devices in order to develop efficient portable sensors with fast response characteristics.

However, the applications of graphene are limited due to the expensive nature of its mass production. Graphene and graphene-related materials are mostly conductors or insulators. So, an uphill task of the graphene research community is to produce semiconducting graphene material for sensor and other electronic applications. Of course, there has been substantial progress in this direction and doping of graphene by metal ions has been successfully achieved. However, the major contribution has been achieved through chemical modifications of graphene molecules, mostly by composite formation. Graphene-metal oxide hybrid composite (GMO) is one such example [2–7]

for electrical and electrochemical applications including chemical sensors, storage, photo catalysis, photovoltaic, and fuel cells as in Figure 1.

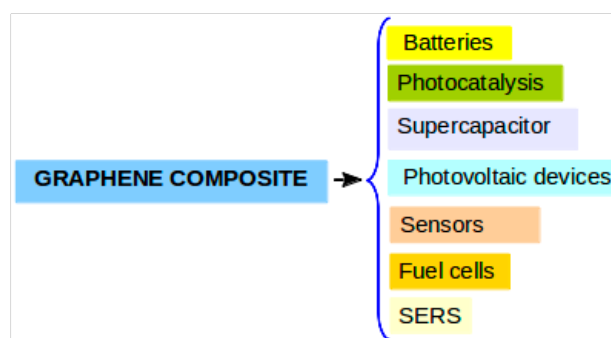


Figure 1. Application of graphene based composites.

GMO has some advantages that can make it easier to scale up than graphene. Since GMO is semiconducting, it can necessarily control the electrical current of a strong conductor such as graphene. Therefore, all the three aspects of electrical conductivity e.g., conducting, semiconducting, and insulating characteristics are available in the carbon family which offers great compatibility for electronic applications.

GMO consists of carbon nanotubes (graphene rolled into a cylinder) decorated with metal oxide nanoparticles. This hybrid material can make high-performance and inexpensive sensors. The real challenge is to explain the sensing behavior of the hybrid material and this requires the knowledge of which molecules are attaching to the nanotube surface which is already itself attached to the metal oxide of the composite. Study in depth of high resolution transmission electron microscopy (HRTEM) and IR imaging can offer “not only the high-definition image of the sensor structure but also a chemical signature identifying the interacting atoms during sensing”. A combination of physics, chemistry, and materials science along with the expertise of surface characterization tools can unfold the actual mechanism of chemical sensing by GMO. It is worth mentioning that the other two derivatives of graphene like graphene oxide and reduced graphene oxide are also equally important for producing nanocomposites with metal oxides for chemical sensor applications. Therefore, in this article we use the terminology “GMO” to denote nanocomposites of graphene, graphene oxide, and reduced graphene oxide.

Recent literature has shown that the sensor applicability of graphene can be made relatively more versatile by the incorporation of other gas sensitive materials like metal oxides in the graphene matrix. Particularly, the development of easy preparation methods for graphene like materials, such as highly reduced graphene oxide *via* reduction of graphite oxide offers a wide range of possibilities for the preparation of graphene based inorganic nanocomposites by the incorporation of various functional nanomaterials for a variety of applications. This is due to the fact that the excellent properties of graphene like thermal and electrical conductivity and structural properties *etc.* can be easily harnessed to maximum extent by developing graphene-based composites [8]. The choice of the second material for composite fabrication depends on the type of application. For chemical gas sensor applications, certain inherent problems like insensitivity of pristine graphene can be tackled either by doping or composite formation. As a result graphene-metal oxide nanocomposites are showing promise in the area of chemical sensing. Other application areas of graphene composites, already illustrated in Figure 1, are photovoltaic, super capacitors, fuel cells, photo catalysis, *etc.* [9–12]. In this article the synthesis and characterizations of the graphene-oxide nanocomposites, along with their sensor response are highlighted with special reference to the basic sensing mechanism. We have selected a few sensor configurations of graphene-oxide nanocomposites amongst the large number of works to discuss the sensing mechanism in detail and we have cited more references of other reports.

2. Synthesis and Characterization of Graphene Based Nanocomposites

Graphene can be synthesized by several methods. Different methods have been reported to produce graphene on a small scale. The simplest methodology is the “scotch-tape method” [13] used for freeing graphene layers from graphite. Other synthesis methods used for research purposes are exfoliation methods [13,14], chemical vapor deposition (CVD) [15], pyrolysis [16], chemical synthesis [17], arc discharge [18], unzipping of CNT [19], solvothermal [20], epitaxial growth [14], molecular beam epitaxy [21], and electrically-assisted synthesis [22]. Exfoliation is a convenient technique to synthesize graphene. The exfoliated graphene layer can be transferred to any medium or substrate for composite formation. For large area graphene, silicon carbide wafers can be thermally treated to generate 2D graphene [23]. Basically the heat helps to eliminate the silicon atoms from the wafer, and thus the left over carbon forms the hexagonal network, which is graphene. Chemical vapor deposition (CVD) is another technique to grow graphene films on the substrate. In this method the substrates are coated with a catalytic metallic (like copper) layer prior to graphene growth, and this layer helps to generate the carbon species when the substrates are exposed to precursor molecular flux [24]. Other metals like nickel, silver, gold, platinum, and cobalt can be used as the catalytic metal [25]. Also both low and high temperature CVD can be employed for graphene growth.

Oxides of graphene are important materials and can be used instead of pure graphene for nanocomposite formation. The oxide of graphene can be easily synthesized by Hummer’s method [26,27]. It requires graphite flakes, nitrates (like sodium nitrate), concentrated acid (like sulfuric acid), permanganate, and deionized water. The components are mixed under stirring conditions in an ice bath to quench the reaction heat. This mixture is then treated with H₂O₂ for an optimized time period. Afterwards, the mixture is cleaned with deionized water by repeated centrifugation followed by filtration. The resulting wet powders of graphene oxide are vacuum dried. The purchased commercial graphene oxide can also be used for nanocomposite preparation.

The second important component in the graphene-oxide nanocomposite is the metal oxide (normally in the form of nanoparticles), which can be easily prepared from metal-organic precursors in suitable acidic or basic pH conditions in excellent yield with controlled size. Another convenient technique to prepare oxide nanoparticles is to start with metallic powders. For example, metallic zinc powder is the source precursor for the synthesis of zinc oxide in an alkaline medium (KOH), in which the metal hydroxide releases its water to form the oxide. Very fine oxide nanoparticles can be obtained by this technique (~14 nm) [28]. Using this method the graphene-oxide composites can be synthesized at room temperature. With the graphene sheets immersed in the solution, the oxide nanoparticles become deposited on the graphene to form the oxide-graphene nanocomposite. The choice of the oxide is very important for the synthesis of oxide based graphene nanocomposites. Normally oxides are gas sensitive materials. However, perfect stoichiometric oxides may not be suitable for sensing due to high resistivity and lack of surface active sites. Hence the optimization of process parameters is quite significant for the synthesis of oxides and the resulting composites. Oxide nanoparticles are preferred to prepare graphene-oxide nanocomposites because nanomaterials have the potential to enhance the gas response due to the very high active surface area. Moreover the low conductivity of oxide materials can be compensated by the considerably high conducting properties of graphene. Hydrothermal technique is quite convenient to develop graphene-oxide nanocomposites. In this method normally the oxide nanoparticles and graphene (Gr) (or graphene oxide (GO) or reduced graphene oxide (rGO)) are synthesized separately, and stored as dispersions in aqueous solution. Thereafter, the aqueous dispersions are sonicated, mixed in the required proportions, and the resulting mixed dispersion is heat treated in a closed ambient. The heat treatment is done slowly and it requires a considerably long time period. After heat treatment the composite is washed with ethanol and dried at relatively low temperatures for 12–24 h. Hydrothermal synthesis of metal oxide-graphene oxide nanocomposite has been already reported [29–31]. The last drying step can sometimes be modified by freezing the yield and then drying, which is termed freeze-drying [32]. A similar technique known as colloidal blending technique is used where both graphene oxide and metal oxide are dispersed in

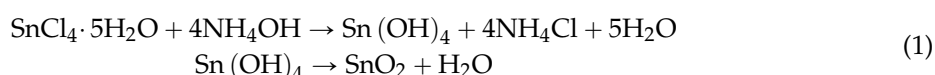
aqueous solutions for intimate mixing and sonicated for a long time (10–12 h) at room temperature. Then the solution is filtered and the composite is dried in vacuum [33].

Clay is an important material, and can be intercalated between graphene oxide layers to form the nanocomposite. The oxygen of graphene oxide can be removed to a large extent by post fabrication annealing [34,35]. A porous network can be created by eliminating a major amount of the clay material at a later stage and such porosity can help to increase gas adsorption by the manifold during gas sensing. However, a suitable clay leaching technique needs to be chosen for this purpose.

Other techniques like solvothermal and mechanochemical intercalation have been used to synthesize graphene composites with ZnO and silica respectively [36,37]. Self assembly is another very successful technique to develop graphene-oxide nanocomposites [38]. In order to prepare SnO₂-graphene composite the functionalized graphene is prepared by mixing graphitic oxide and aqueous sodium 1-dodecanesulfonate (surfactant) at a particular temperature (<100 °C). The oxide component was introduced by mixing SnCl₂ in HCl solution and adding the solution into the as-prepared graphene-surfactant mixture under stirring conditions. Then urea and H₂O₂ are added. Finally, water is added to dilute the solution and the mixture is maintained at 90 °C for 12–16 h. The resulting solution is cleaned by repeated centrifugation and the wet powders are vacuum dried at 50–70 °C overnight. The dried powders can be calcined in H₂/Ar ambient at 400 °C as per requirement. Such a self assembly technique can also be used for developing NiO-graphene, MnO₂-graphene, and mesoporous graphene-SiO₂ nanocomposites.

Many other methods like solvent-exfoliation or *in situ* growth of TiO₂ nanoparticles on graphene oxide nano-sheets by liquid phase deposition, followed by annealing/firing at 200 °C, have been reported to develop graphene-TiO₂ nanocomposites or graphite oxide/TiO₂ composites, for photo catalytic applications [39–41].

Reduced graphene oxide and tin oxide nanoparticles were used to develop nanocomposite by a facile hydrothermal technique [42]. The precursors used were 0.4 mg GO dispersed in water, 0.35 g of SnCl₄·5H₂O dissolved in water, and 0.1 M ammonia solution. The reaction was carried out for 4-h at 160 °C. The tin chloride molecules attach themselves onto the reduced graphene surface and eventually tin dioxide is formed via Equation (1). Probably the reduced graphene surface provides heterogeneous nucleation sites.



Generally, X-ray diffraction (XRD), scanning electron microscopy (SEM), and transmission electron microscopy (TEM) are the essential tools to determine the crystallinity, particle size, and morphology of the nanostructures. In the present study, most of the oxide nanoparticles and graphene or graphene oxide nanostructures have been characterized by the three techniques mentioned above. The XRD spectra of the metal oxide, graphene, graphene oxide or reduced graphene oxide are different from the corresponding composites due to the peak shift. If there is no extra peak (or peaks) observed in the XRD spectra the purity of the composite can also be determined. While SEM provides information of the overall morphology within the limit of its resolution the TEM (also HRTEM) study can give the vision of the detailed morphology of the individual as well as composite nanostructures.

Tin dioxide-reduced graphene oxide nanocomposites were characterized by XRD, SEM, and TEM [42]. The X-Ray diffraction peaks of the composite are mostly from SnO₂. However, a very small peak from rGO at 25.5° is observed in the composite XRD spectra Figure 2. Most of the peaks in the nanocomposite are from SnO₂, and only one is from rGO as revealed in Figure 2. The EDS results shown in Figure 3 clearly reveal that only the elements carbon, oxygen, and tin are present in the system. This also indicates the purity of the nanocomposite.

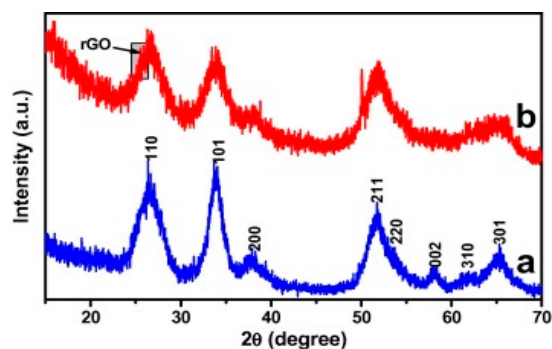


Figure 2. X-ray diffraction (XRD) spectra of (a) SnO₂ and (b) rGO-SnO₂ nanocomposite [42].

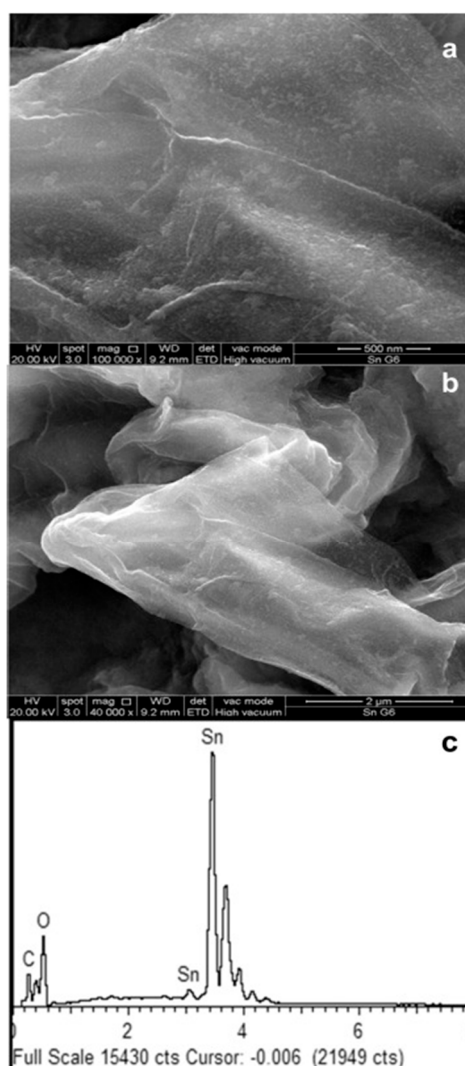


Figure 3. (a) Low magnification field emission scanning electron microscopy (FESEM) image of rGO-SnO₂ nanocomposite (b) high magnification FESEM image; and (c) energy dispersive spectrum (EDS) of rGO-SnO₂ nanocomposite [42].

The morphology of the nanocomposite was analyzed by TEM, which revealed the oxide nanoparticles (of ~10 nm) on the reduced graphene oxide surface similar to the morphology revealed by field emission SEM study Figures 3 and 4. Irregular SnO₂ nanoparticles were found to be uniformly deposited on the graphene layer.

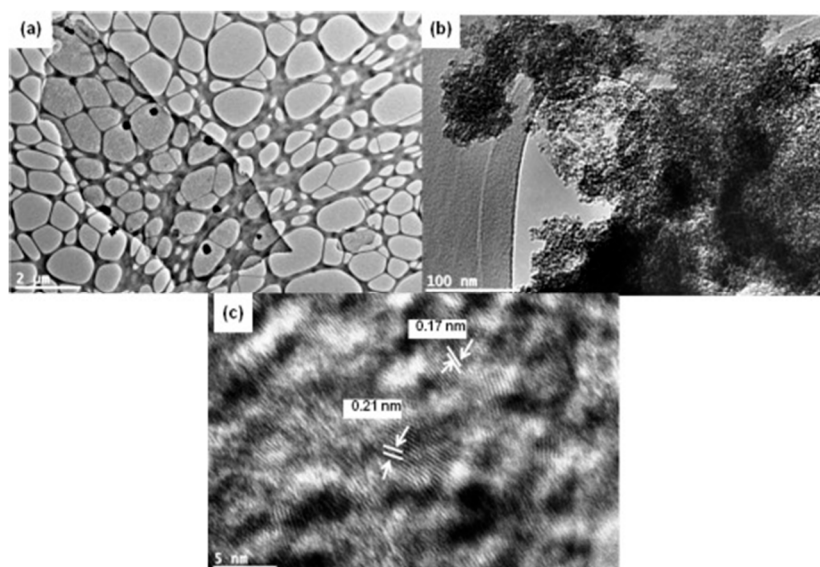


Figure 4. (a) Low-magnification transmission electron microscopy (TEM) image of rGO-SnO₂ nanocomposite (b); and (c) are high resolution transmission electron microscopy (HRTEM) images of rGO-SnO₂ nanocomposite showing lattice spacing of 0.17 nm [42].

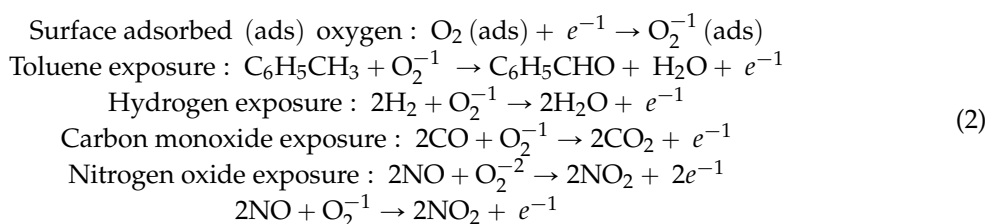
Raman spectra of individual components and the composite can reveal characteristic information about the defects/disorders and about the bonds. Normally the D-peak denotes the defects, while the G-peak and 2D peaks are for the sp² hybridized carbon network and presence of impurities in graphene respectively. For graphene, usually the Raman peaks correspond to D- (~1323 cm⁻¹), G- (~1573 cm⁻¹), and 2D- (~2657 cm⁻¹) bands [43].

For a graphene-oxide composite, the band positions can shift relative to the peaks of the pure spectrum, or the shape of the peaks can be different. Also, the oxide bands at relatively lower wave numbers indicate the nature of bonding in the oxides. Sometimes, due to arbitrary stretching the bands can shift towards either lower or higher wave numbers. The interaction between the components of the composite can also be determined by FTIR (Fourier Transform Infra-Red) spectroscopy.

3. Mechanism of Gas Sensing and Device Fabrication

Normally, the gas sensitivity of graphene-metal oxide nanocomposite is controlled by both the components. While pristine graphene may not respond to the sensing gases, graphene oxide and reduced graphene oxide can trap analyte gas molecules and bring a change in the conducting properties. Usually reduced graphene oxide has better conducting properties than graphene oxide due to non-stoichiometry. Hence the response characteristics of the composite can be controlled by either of the oxides or by both. Normally oxidizing and reducing gases have different interactions, which can lead to carrier generation or carrier annihilation in the sensing layer. This leads to a change in the device resistance or current, which can be monitored as the sensor signal. In the absence of catalytic components (like palladium, platinum, *etc.*) the presence of surface adsorbed oxygen is necessary to act as a good sensing platform. The surface oxygen remains in the charged state by accommodating an electron from the matrix during adsorption. The surface activity varies according to the availability of surface unsaturated bonds which depends on the process of material synthesis. If these unsaturated bonds are covered by molecules like oxygen the surface activity is reduced and there is a possibility of charge sharing during the surface coverage. Upon exposure to the sensing gases the dangling oxygen radicals interact with the gas/vapor molecules and release trapped electrons. During sensing the analyte gases (maybe reducing or oxidizing) come into contact with the so called passive surface and surface oxygen is removed. During these interactions, electrons can either be released or trapped depending on the conductivity of the base matrix. During the sensor recovery process, such sites

are re-occupied by oxygen available in the surrounding carrier stream. For example, some simple interactions are outlined below (Equation (2)):



Depending on the nature of the conductivity of the sensing matrix (either n-type or p-type) the current increases or decreases during sensing. The availability of the charged oxygen radicals is sufficient with both the metal oxide nanoparticles/clusters and graphene oxide or reduced graphene oxide. Hence the sensing can be controlled by both. Therefore, the cumulative contributions from both metal oxide and graphene/graphene oxides may increase the device response by the manifold. It is well known that the catalytic metal enhances the solid-gas interaction to a large extent and it may be chosen depending on the nature of the analyte gas. For example, palladium is the best choice for hydrogen and nickel is more appropriate for carbon monoxide. Palladium has excellent affinity for hydrogen even at room temperature and it adsorbs hydrogen to a large extent. Subsequently, hydrogen molecules dissociate into hydrogen atoms [44]. On the other hand, nickel is appropriate for sensing carbon monoxide because of its tendency to form nickel carbonyl with carbon monoxide with relatively low activation energy [45]. However, cross sensitivity is indeed a standing problem for chemical sensing and 100% selective response is difficult to achieve. Therefore, some level of cross sensitivity always exists despite the use of catalytic agent. The incorporation of the catalytic component can improve the response behavior of the nanocomposite for a specific gas along with the low extent of cross-sensitivity.

Parallel metallic electrodes can be printed (or deposited) on the composite film (thin or thick) to develop a simple resistive device (Figure 5).

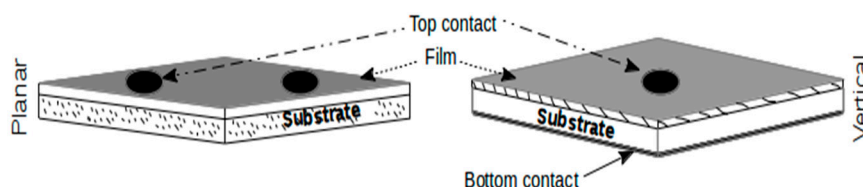


Figure 5. Resistive and dot contact device configuration.

To develop the miniaturized sensor configuration with reproducible characteristics the dot contact resistive devices (shown in Figure 5) are fabricated with the catalytic metal contact on the composite thin films. If the composite material is obtained in powder form during synthesis, the sensor film is prepared by using the following procedure. The powder is dispersed in aqueous solvent by sonication. Then a flexible thin porous polymer like porous polyvinylidene fluoride (PVDF) membrane is rolled and fitted just like a filter paper inside a funnel. The dispersed solution is poured into the funnel and the liquid is eliminated using positive suction from an attached pump. As the liquid escapes through the pores the powder particles become trapped on the surface of the membrane which is removed and baked for 2–3 h. Then the composite layer can be carefully peeled off the membrane. The prerequisite for peeling is that the inter particle binding of the composite should be good; otherwise the layer can break into pieces. A binder can be used to solve this problem but it can create the following problem. If the binder is not removed completely during baking or if the burnt residue remains in the composite, the resulting film is likely to be contaminated and may deteriorate the device performance. Therefore, further study is necessary to consider this particular aspect. We know that both graphene or graphene

oxide and the metal oxide of the nanocomposite are resistant to high temperature. However, for the application of the composite film prepared by this method the maximum sensing temperature will be determined by the temperature stability of the membrane. Therefore, for high temperature operation, flexible and thin porous non-interfering ceramic substrates can be used instead of polymer membrane. Also the composite films can be developed by modifying the graphene films with oxide nanoparticles (by solution dipping) followed by baking for sufficient time. The composite powders in the pellet form can also be used for device fabrication.

Atomic Layer Deposition (ALD) can be deployed to deposit a layer (or scattered clusters) of metal oxide on the functionalized graphene surface on a substrate [46]. First, the graphene/graphene oxide is transferred onto the substrate and then the metal oxide layer can be deposited by ALD. Finally the substrates can be annealed in a controlled ambient for a long period of time to develop a composite morphology. CVD grown graphene on oxidized silicon wafers can also be used for this purpose. Such composites deposited on a substrate are very useful for sensor device fabrications (both planar and vertical devices).

4. Sensor Response of the Metal Oxide-Graphene Nanocomposites

Generally a fiber optic assembly is more suitable for low temperature operation. Hence the fiber optic sensors show appreciably high response in the low temperature domain. Chemo resistive devices with metal oxide-graphene nanocomposite can be fabricated for efficient optical sensor applications if the nanocomposite is sensitive at low temperature.

Kaolin-graphene oxide nanocomposite was reported as a good sensing material for the detection of gases/vapors like NH₃ and HNO₃ [47]. The improved conductivity of the nanocomposite was obtained after thermal annealing. The composite samples, which were heat treated at 400 and 600 °C showed appreciably good sensitivity to NH₃ and HNO₃. The response was relatively better in comparison to the response of only annealed GO samples. The enhanced response is attributed to the combined response of reduced GO and Kaolin toward the analyte gas/vapor molecules. The sensing mechanism can be explained with the help of the schematic diagram shown in Figure 6.

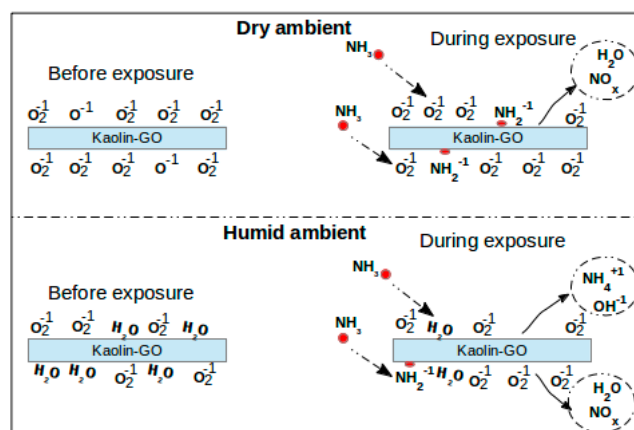
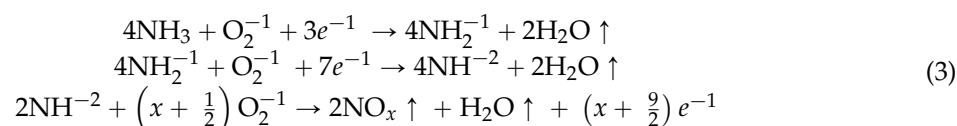


Figure 6. Sensing mechanism for kaolin-GO nanocomposite.

The concept of two different types of solid-gas interaction at the surface can be realized for ammonia sensing. The first interaction is in the presence of moisture and the other one is in the absence of moisture. In the absence of moisture, the sensing proceeds as per Equation (3) shown below:



The reactions presented in Equation (2) will proceed at the active sites. Other charge states of the oxygen radical (like O^{2-} or O^{1-}) can also initiate such reactions. As the ammonia molecule loses its hydrogen atoms one by one, the removal of hydrogen becomes more and more difficult. Actually the increased negative charge concentration of the resultant radicals exerts a strong attractive force on the remaining hydrogen atoms. As a result, the higher activation energy is required for the reactions to proceed and therefore other energy sites might be involved during sensing. In fact, Zhang *et al.* [47] stated the two different adsorption sites as low and high binding energy sites. Normally, sensing is fast from the so called low binding energy sites and the sensing happens due to a single step reaction. However, for multistep reactions, both low and high activation energy sites are involved and the complete recovery can sometimes be a problem due to trapping of the analyte species. This is the reason for continuous drift in the baseline resistance (increase) by the application of successive gas pulses as observed by Zhang *et al.* [47]. Probably the gas desorption from some active sites was incomplete while more desorption was observed from the other active sites.

Another interesting fact that was reported by Zhang *et al.* [47] was the influence of humidity. In their study the normal gas sensing program in dry ambient was interrupted by a pulse of humid nitrogen (without analyte), and then the gas response studies were continued using dry carrier and analyte gases. However, the same authors reported that the nature of gas response pattern remained the same after exposure to humidity again and a shift (slight decrease) in baseline resistance was observed upon exposure to humid nitrogen, Figure 7. In the humid atmosphere the sensing surface gathers moisture molecules. So, it is likely that some trapped analyte (gas or radicals) could be released by water molecules, and the nature of the active site would be reinstated as before. In such a process few electrons are released and eventually decrease the baseline resistance to some extent. However, the change in resistance is governed by how easily such reactions proceed.

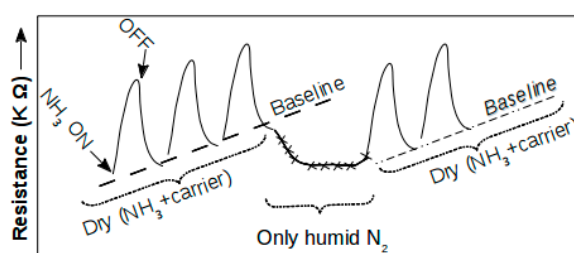
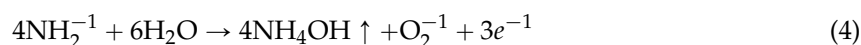
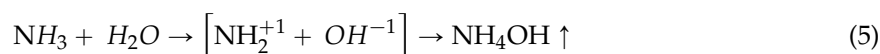


Figure 7. Experimental observations during NH_3 exposure to kaolin-GO composite films along with the interference of humidity.

Zhang *et al.* [47] reported a small change in resistance upon exposure to moisture and it is also supported by Equations (4) and (5).



Also this is further supported by Equation (5)



Hence it can be speculated that if sensing is performed in a humid environment, a relatively less number of ammonia molecules will be available for the generation of electrons following Equation (2) because of the reaction with water. Therefore, it is likely that the response of the composite sensors could be affected in a humid environment.

Graphene- WO_3 nanocomposite is a promising material for sensing NO_2 at room temperature as well as at elevated temperature [48]. In fact the best response towards NO_2 was obtained at $250^\circ C$. Graphene oxide was obtained by Hummers method, and subsequently reduced to graphene in

hydrazine hydrate and ammonia solution. The WO_3 sol was obtained from the reaction of WCl_6 and ethanol in a controlled atmosphere. WO_3 sol was added to graphene sol to make Graphene- WO_3 nanocomposite sol. A drop of the resulting nanocomposite sol was put on a substrate and fired at 600°C for 30 min for the film preparation. Pure graphene and pure WO_3 films were also used for comparative studies. It was observed that the response magnitude of the nanocomposites were higher than the pure films at room temperature. For the pure graphene film, a decrease in resistance was observed at room temperature upon exposure to oxidizing NO_2 gas. Hence the films are p-type conducting. It has already been mentioned above that reduced graphene oxide (rGO) is obtained by reducing graphene oxide (GO). Therefore, the surface sensitivity is most probably due to the unsaturated oxygen bonds. The p-type conductivity of reduced graphene oxide is reported in the literature [49]. WO_3 film is n-type because of its non-stoichiometric character with excess oxygen vacancies. However, the nanocomposites with relatively higher weight concentration of graphene (1%) showed p-type sensor response at both room temperature and elevated temperatures. This could be attributed to the dominance of p-type reduced graphene oxide in the nanocomposite matrix. The sensing mechanism of reduced graphene oxide- WO_3 nanocomposite may be due to the modulation of the inter-grain Schottky barrier in both WO_3 and graphene oxide- WO_3 nanocomposites. The response is better in the nanocomposite than pure WO_3 . The higher surface area of the nanocomposite and relatively higher change in the magnitude of the potential barrier at the graphene- WO_3 interfaces are responsible for the better sensor response characteristics. The barrier change in the nano heterojunction, n- WO_3 /p-graphene oxide of the nanocomposite is responsible for sensing. Therefore, the response of the nanocomposite sensor is better than the sensors based on the individual components. The nanocomposite (with 0.5 wt % graphene) showed the best results at 250°C , probably due to the optimized distribution of n-type and p-type components.

WO_3 -graphene composite was used to sense hydrogen by Esfandiar *et al.* [50]. Palladium was used in this composite to improve the hydrogen adsorption ability. GO and partially reduced graphene oxide (rGO) was used to develop the nanocomposite which was synthesized by Hummer's method and hydrothermal technique respectively. Hydrogen molecules when exposed to Pd- WO_3 /GO and Pd- WO_3 /rGO nanocomposites dissociate to atomic hydrogen which interacts with surface adsorbed oxygen to generate electrons and increase the conductivity.

Graphene based nanocomposites are suitable for the development of a cataluminescence sensor. A basic schematic representation of the cataluminescence sensing set up is shown in Figure 8. These sensors yield luminous light during solid gas interaction. Such a type of sensor was reported first by Breyse *et al.* [51], in 1976. These sensors have normally fast response, good reproducibility, and long-term stability. The cataluminescence sensors are able to detect very low concentration (~ 1 ppm) of the analyte due to the reduced noise level. The sensing intensity of such sensors varies depending on the catalytic activity of the sensing material. The porous morphology of the sensing material is an added advantage of these sensors as the gas (or vapor) molecules can find enhanced surface area for interactions. SnO_2 /graphene composite was used as a cataluminescence sensor for propanol detection [52]. The luminous output was due to the catalytic oxidation of propanol molecules on the composite surface. A very low limit of propanol detection ($0.3\ \mu\text{g}/\text{mL}$) was obtained with these sensors. The cataluminescence sensors can act as selective sensors for the detection of volatile organic compounds because different molecules can have different luminescence signatures.

Room temperature acetone gas sensors based on SnO_2 -r-GO composite film are reported by Zhang *et al.* [53]. The composite was developed by employing hydrothermal methodology, and the device was fabricated on PCB (printed circuit board) substrates by a drop casting technique. These composites showed relatively better efficiency due to the porous nature of the films, nano-heterojunction character, and presence of charged oxygen species (O^{2-}). Similarly, tin dioxide composites have also been reported for gas sensors [54].

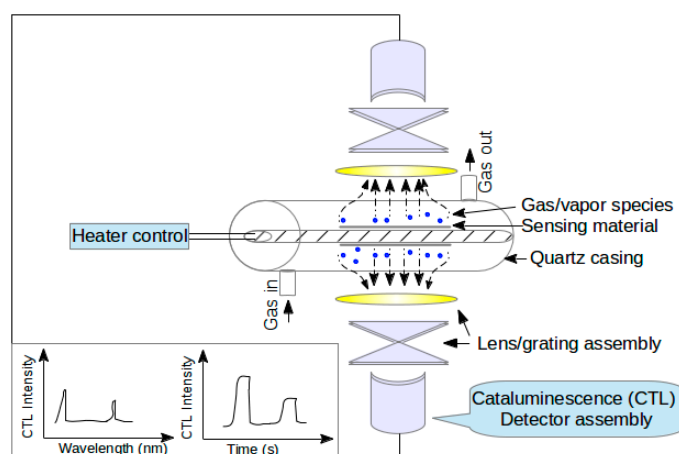


Figure 8. Schematic of cataluminescence sensing assembly.

Graphene oxide and Sn precursor solution were used to synthesize graphene-tin oxide (Gr-SnO₂) nanocomposite by a facile hydrothermal method without adding any surfactant [42]. Formation of Gr-SnO₂ nanocomposite was confirmed by field emission scanning electron microscopy (FESEM), high resolution transmission electron microscopy (HRTEM), X-ray diffraction (XRD), and energy dispersive spectroscopy (EDS). FESEM and HRTEM images showed the homogeneous deposition of SnO₂ nanoparticles with an average particle size of 10 nm on graphene. The Gr-SnO₂ nanocomposite was used to fabricate a modified electrode for the selective detection of dopamine (DA) in the presence of ascorbic acid (AA) by the electrochemical method. The differential pulse voltammetric (DPV) diagram showed the lowest limit of detection of 1 μM of DA in the presence of ascorbic acid (AA). The sensing mechanism is schematically represented in Figure 9. DA is easily oxidized to dopamine quinone (DAQ) (dopamine orthoquinone) by exchange of two electrons. These two electrons become transferred to the electrode and there is variation of the current.

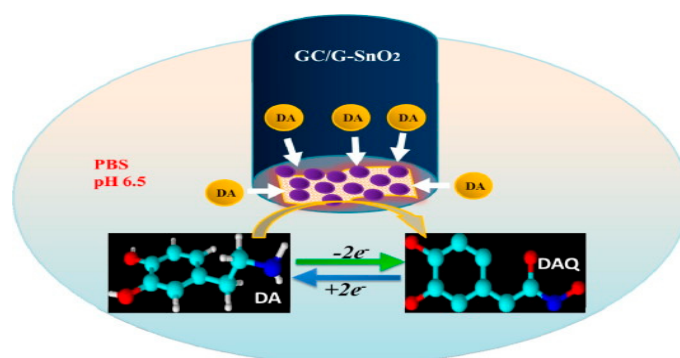


Figure 9. Schematic of dopamine sensing with graphene-SnO₂ nanocomposite [42].

SnO₂-reduced graphene oxide quantum dots were synthesized from tin chloride by the hydrothermal technique in the presence of a surfactant [55]. These sensors were sensitive to 500 ppm hydrogen (89.3%) and also liquefied petroleum gas (LPG) (92.4%) at 200 and 250 °C respectively.

Graphene/ZnO quantum dot composite has been studied for sensing LPG at fairly low concentrations (<1 ppm) [56]. The chemiresistive sensor showed an increase in response with increasing LPG concentrations. The study was extended with pristine graphene and ZnO separately and showed lower sensing response than the composite. The detection of LPG was explained as due to the formation of H₂O and CO₂ by surface reaction of the adsorbed oxygen.

Simple resistive devices were also fabricated with graphene-zinc oxide nanocomposite paste, by developing thick films on alumina substrates (with gold electrodes) [57]. Graphene-zinc oxide

nanocomposite was synthesized by reducing zinc acetate and graphene oxide (GO). GO was obtained by Hummer's method. The graphene content in the nanocomposite was varied, and the composite with 1.2 wt % of graphene showed better response towards hydrogen at an optimized temperature of 150 °C. The sensing efficiency of these composites was better than bare ZnO response.

Another simple resistive device was developed with ZnO-reduced graphene oxide (rGO) for detection of acetylene gas. Silver (Ag) was incorporated in ZnO-rGO composite chemically [58]. The device resistance changes during the interaction with analyte gas molecules and electrons are released during such interactions. The release of electrons is attributed to the reactions between a surface adsorbed oxygen species and acetylene molecules. Different types of oxygen radicals were reported by Iftekhhar *et al.* [58]. For low temperatures (<100 °C), O_2^- plays the dominant role in sensing. For moderate temperatures (between 100 and 300 °C), O^- radicals take active part in sensing, while at relatively higher temperatures (>300 °C), double charged oxygen [O^{2-}] is available. In this study, the presence of silver ensures better oxygen activity (in addition to ZnO) of the composite.

Thin films of ZnO have also been deposited on graphene films by Atomic layer Deposition (ALD) for sensor applications [59]. Such sensors were sensitive to formaldehyde vapors, and the performance was relatively better in comparison to pure ZnO or graphene. ZnO nanowires have been used with GO for the purpose of sensing [60]. These sensors were sensitive to ethanol, and the large surface of the nanocomposite produced high response.

In addition to the conventional methods of composite fabrication, ZnO particles were synthesized at low temperature and were anchored to the surface of graphene oxide sheets via a simple and fast method to produce the composite material [61]. UV-visible spectrophotometry and FT-IR spectroscopy were used to characterize ZnO and graphene oxide. The morphology of ZnO, graphene oxide, and their distribution in the composites matrix was studied by FE-SEM and Bio-AFM images. The current-voltage results showed that the electrochemical properties of the composites were superior to the individual components. The composites also demonstrated excellent antibacterial properties which can be utilized for applications in antibacterial medicine. The ZnO/graphene oxide composites fabricated by this method can be used for super-capacitance, biosensors, and disinfectants.

Different microscopic techniques have been deployed to reveal the surface morphology and uniformity of the composites. Spectroscopic techniques have been used to investigate the quality of the as-synthesized powder samples as well as the extent of graphitization of the samples. Gas-sensing properties of the rGO and Zn-GO nanocomposite samples have been reported by designing and fabricating coil sensors with two Pt terminals and a heating element. Reduced graphene oxide-ZnO nanocomposite powders synthesized by a simple hydrolysis method followed by annealing in ambient N_2 gas have been reported [62]. By using hydrazine hydrate as the reducing agent to graphene oxide and subsequent decoration by ZnO nanoparticles the nanocomposite was produced. The ZnO-rGO nanocomposite displays more promising and better NO_2 gas sensing properties than the pristine rGO. The nanocomposite exhibited a response of ~32% for 50 ppm NO_2 at as low a temperature as 50 °C. This work suggested that a potential low-power portable NO_2 sensor can be fabricated using Zn-rGO nanocomposite material.

Titanium dioxide has also been harnessed to develop nanocomposite with graphene. Such composites have gained prominence for sensing applications due to graphene, its exotic forms, and various characteristics of TiO_2 like high temperature stability *etc.* Also the extraordinary electrical conductivity and large surface to volume ratio of such composites are added advantages for chemical sensing.

Dopamine (DA) is an important neurotransmitter of the central nervous system that controls a lot of physiological functions. A graphene (rGO)- TiO_2 nanocomposite can be used to detect DA due to the good electron transfer characteristics of the composite and its ability to distinguish DA from other interfering compounds [63]. The sensors were prepared by putting a drop of the graphene- TiO_2 nanocomposite on a glassy carbon electrode (GCE) and drying in air at 60 °C for 30 min. For comparative studies pure TiO_2 and pure rGO electrodes were also developed. The electrochemical

sensing was done in a cell having the GCE soaked with a drop of nanocomposite (as the working electrode), platinum wire (as the counter electrode), and a saturated calomel electrode (SCE) (as the reference electrode). The electrolyte used was a 0.1 M phosphate buffer solution (pH 6.5). For the case of nanocomposite, the anodic current was found to increase with the increase in DA concentration. The limit of detection of DA was 1.5 μM . Basically DA gets oxidized on the composite impregnated GCE and forms dopamine quinone (DAQ). Upon the application of a potential to the electrode, the transformation of DA to form DAQ happens with exchange of two electrons and two protons. These electrons are collected by the electrode and hence the current increases. Also this nanocomposite-laden GCE was able to selectively determine DA in presence of ascorbic acid. The electro catalytic activity of the GCE with nanocomposite was higher in comparison to pure TiO_2 and pure rGO electrodes. Similar dopamine sensors based on TiO_2 -graphene composite have been reported [64,65].

Jang *et al.* [66] developed a sensitive glucose biosensor using a three-dimensional silver-graphene-titanium dioxide (3D Ag-Gr- TiO_2) composite electrode. A colloidal mixture of a silver acetate precursor ($\text{C}_2\text{H}_3\text{AgO}_2$), graphene oxide, and TiO_2 nanoparticles was prepared by an aerosol spray pyrolysis method to synthesize the 3D Ag-Gr- TiO_2 composite. The particle morphology of the 3D Ag-Gr- TiO_2 composites was spherical in shape and the average size was 0.45 to 0.64 μm as controlled by changing the process variables. Operating temperature, gas flow rate, and TiO_2 concentration had influence on the particle properties as obtained from the investigation. Following a reduction process Ag nanoparticles of a size less than 10 nm were deposited on the surfaces of both TiO_2 and Gr. Cyclic voltammetric measurements were employed to characterize the glucose biosensor fabricated from the as-prepared 3D Ag-Gr- TiO_2 composite with the highest sensitivity of 12.2 $\mu\text{A}/\text{mM}\cdot\text{cm}^2$.

Reduced graphene oxide/titanium dioxide nanocomposites have been synthesized by a simple hydrothermal technique [67]. The titanium dioxide and graphene oxide nanoparticles were formed at the same time using a single-stage approach. The triethanolamine used in this process acts as a reducing agent for the graphene oxide and also as a capping agent for the formation of titanium dioxide nanoparticles with a narrow size distribution (~ 20 nm). The uniform distribution of the nanoparticles on the reduced graphene oxide nanosheets was verified by transmission electron micrographs. Also the thermal stability of the composites was studied by thermogravimetric analysis. The use of a reduced graphene oxide/titanium dioxide nanocomposite-modified glassy carbon electrode was demonstrated by interacting with mercury(II) ions in potassium chloride electrolyte and an improvement in performance was observed compared to a conventional glassy carbon electrode (GCE).

In another study MnO/C nanocomposite electrodes were prepared by dipping conducting Ni foam or Ti foil into Mn-oleate/hexane solution for a long period so that the solvent evaporates at room temperature [68]. Then the conducting substrates were heat-treated at 550 $^\circ\text{C}$ in Ar ambient for 2 h. These electrodes were used to detect hydrogen peroxide (H_2O_2) galvanostatically in the voltage range 0.01–3.0 volts using Ag/AgCl reference electrode for bio based applications related to tumor cells. The sensor study was carried out with H_2O_2 , slowly added to 5 mL phosphate buffered solution (PBS). Appreciable change in current density was observed in the presence of H_2O_2 and the conductance change attained equilibrium within a 5–10 s time period. The detection limit for these sensors is 2 μM .

Other graphene based composites like graphene-mica and graphene- SiO_2 have been reported to be useful for sensing gases like ammonia. Apart from binary composites between oxide and graphene, ternary composites between polymer, oxide, and graphene have also been reported [69]. Polypyrrole, titanium dioxide nanoparticles, and graphene nanoplatelets (GN) were used to generate the composite. The size of TiO_2 nanoparticles was in the range 10–30 nm. This ternary composite showed relatively higher sensitivity to ammonia in comparison to GN and polypyrrole-GN combination. Similarly, another ternary composite (rGO-CNT- SnO_2) was used to detect NO_2 at room temperature with sensitivity as low as 1–100 ppm of NO_2 with a response time of 8 s [70]. The composites like $\text{Co}(\text{OH})_2$ -rGO have been used to detect NO_x gas [71]. There are other reports of NO_2 sensors based on

graphene and tin oxide composites [72,73]. Fe₂O₃ and MoO₃ have been used to develop composites with graphene and rGO to detect H₂S [74,75].

5. Conclusions and Future Outlook

Graphene with its excellent structural, chemical, electronic, and electrical properties is the obvious choice for future sensor applications. Also graphene and graphene oxide based hybrid composites with metal oxides are the next generation materials for chemical and biosensors for versatile sensing applications [76,77]. The present day nanotechnology and its compatibility with graphene and its derivatives are an added advantage for the development of efficient and much faster sensor devices as chemical and bio sensors. Particularly for gas sensor applications, graphene nanocomposites have shown immense promise for the development of reliable and selective sensor devices in miniaturized dimensions with long term stability. Graphene, graphene oxide (GO) and reduced graphene oxide (rGO) when mixed with metal oxides produce potential composite materials with a great promise for large scale production of selective chemical and biosensors for cost effective applications in the areas of environmental pollutions, safety and security, and clinical and pharmacological analysis. The present review article focuses on the synthesis, characterizations and sensor performance of the nanocomposites of metal oxides and graphene and/or other graphene derivatives. Different synthesis methods of these nanocomposites have been discussed. An attempt has been made to analyze the sensing mechanism for different gases/vapors. Functionalities like oxygen radicals play the major role during sensing. Finally the performance of different graphene-oxide nanocomposites for sensing gases and vapors has been presented. While resistive devices based on oxide-graphene composites are useful for chemical sensing, junction devices are also suitable for the same purpose. The superior solid-analyte interactions for all types of sensors with oxide-graphene nanocomposites are possible due to the large surface to volume ratio. Polymers are also attractive candidates for synthesizing composites with graphene and its derivatives. These composites have ample scope for surface functionalization and modulation of their electrical and optical properties, which render wide applications of polymer-graphene nanocomposites in the field of chemical sensors. Metal-graphene composites are also suitable for chemical sensor applications.

To conclude, graphene based nanocomposites have immense potential in the coming decade. Such materials will manifest not only excellent chemical sensitivity with fast response and recovery, but also develop a unique configuration with versatile applications in a combined sensor platform. Last but not least, it is expected that more sophisticated sensing mechanisms will explain the operations of these superior chemical sensor devices.

Conflicts of Interest: The authors declare no conflict of interest.

References

1. Basu, S.; Bhattacharyya, P. Recent developments on graphene and graphene oxide based solid state gas sensors. *Sens. Actuators B* **2012**, *173*, 1–21. [[CrossRef](#)]
2. Anasori, B.; Beidaghi, M.; Gogotsi, Y. Graphene—Transition metal oxide hybrid materials. *Mater. Today* **2014**, *17*, 253–254.
3. Sun, M.; Liu, H.; Liu, Y.; Qu, J.; Li, J. Graphene-based transition metal oxide nanocomposites for the oxygen reduction reaction. *Nanoscale* **2015**, *7*, 1250–1269. [[CrossRef](#)] [[PubMed](#)]
4. Zhang, W.; Liu, F.; Li, Q.; Shou, Q.; Cheng, J.; Zhang, L.; Nelson, B.J.; Zhang, X. Transition metal oxide and graphene nanocomposites for high-performance electrochemical capacitors. *Phys. Chem. Chem. Phys.* **2012**, *14*, 16331–16337. [[CrossRef](#)] [[PubMed](#)]
5. Khan, M.; Tahir, M.N.; Adil, S.F.; Khan, H.U.; Siddiqui, M.R.H.; Al-warthan, A.A.; Tremel, W. Graphene based metal and metal oxide nanocomposites: Synthesis, properties and their applications. *J. Mater. Chem. A* **2015**, *3*, 18753–18808. [[CrossRef](#)]
6. Hu, C.; Lu, T.; Chen, F.; Zhang, R. A brief review of graphene–metal oxide composites synthesis and applications in photocatalysis. *J. Chin. Adv. Mater. Soc.* **2013**, *1*, 21–39. [[CrossRef](#)]

7. Joshi, M.K.; Pant, H.R.; Kim, H.J.; Kim, J.H.; Kim, C.S. One-pot synthesis of Ag-iron oxide/reduced graphene oxide nanocomposite via hydrothermal treatment. *Colloids Surf. A Physicochem. Eng Asp.* **2014**, *446*, 102–108. [[CrossRef](#)]
8. Stankovich, S.; Dikin, D.A.; Dommett, G.H.B.; Kohlhaas, K.M.; Zimney, E.J.; Stach, E.A.; Piner, R.D.; Nguyen, S.B.T.; Ruoff, R.S. Graphene-based composite materials. *Nature* **2006**, *442*, 282–286. [[CrossRef](#)] [[PubMed](#)]
9. Huang, X.; Qi, X.; Boey, F.; Zhang, H. Graphene-based composites. *Chem. Soc. Rev.* **2012**, *41*, 666–686. [[CrossRef](#)] [[PubMed](#)]
10. Zhang, K.; Zhang, L.L.; Zhao, X.S.; Wu, J.S. Graphene/polyaniline nanofiber composites as supercapacitor electrodes. *Chem. Mater.* **2010**, *22*, 1392–1401. [[CrossRef](#)]
11. Paek, S.-M.; Yoo, E.; Honma, I. Enhanced cyclic performance and lithium storage capacity of SnO₂/graphene nanoporous electrodes with three-dimensionally delaminated flexible structure. *Nano Lett.* **2009**, *9*, 72–75. [[CrossRef](#)] [[PubMed](#)]
12. Williams, G.; Seger, B.; Kamat, P.V. TiO₂-graphene nanocomposites, UV-assisted photocatalytic reduction of graphene oxide. *ACS Nano* **2008**, *2*, 4348–4350. [[CrossRef](#)] [[PubMed](#)]
13. Novoselov, K.S.; Geim, A.K.; Morozov, S.V.; Jiang, D.; Zhang, Y.; Dubonos, S.V.; Grigorieva, I.V.; Firsov, A.A. Electric field in atomically thin carbon films. *Science* **2004**, *306*, 666–669. [[CrossRef](#)] [[PubMed](#)]
14. Park, S.; Ruoff, R.S. Chemical methods for the production of graphenes. *Nat. Nanotechnol.* **2009**, *4*, 217–224. [[CrossRef](#)] [[PubMed](#)]
15. Reina, A.; Jia, X.; Ho, J.; Nezich, D.; Son, H.; Bulovic, V.; Dresselhaus, M.S.; Kong, J. Large area, few-layer graphene films on arbitrary substrates by chemical vapor deposition. *Nano Lett.* **2009**, *9*, 30–35. [[CrossRef](#)] [[PubMed](#)]
16. Campos-Delgado, J.; Romo-Herrera, J.M.; Jia, X.; Cullen, D.A.; Muramatsu, H.; Kim, Y.A.; Hayashi, T.; Ren, Z.; Smith, D.J.; Okuno, Y.; *et al.* Bulk production of a new form of sp² carbon: Crystalline graphene nanoribbons. *Nano Lett.* **2008**, *8*, 2773–2778. [[CrossRef](#)] [[PubMed](#)]
17. Tung, V.C.; Allen, M.J.; Yang, Y.; Kaner, R.B. High-throughput solution processing of large-scale graphene. *Nat. Nanotechnol.* **2009**, *4*, 25–29. [[CrossRef](#)] [[PubMed](#)]
18. Li, N.; Wang, Z.; Zhao, K.; Shi, Z.; Gu, Z.; Xu, S. Large scale synthesis of N-doped multi-layered graphene sheets by simple arc-discharge method. *Carbon* **2010**, *48*, 255–259. [[CrossRef](#)]
19. Elías, A.L.; Botello-Méndez, A.R.; Meneses-Rodríguez, D.; González, V.J.; Ramírez-González, D.; Ci, L.; Muñoz-Sandoval, E.; Ajayan, P.M.; Terrones, H.; Terrones, M. Longitudinal cutting of pure and doped carbon nanotubes to form graphitic nanoribbons using metal clusters as nanoscalpels. *Nano Lett.* **2010**, *10*, 366–372. [[CrossRef](#)] [[PubMed](#)]
20. Choucair, M.; Thordarson, P.; Stride, J.A. Gram-scale production of graphene based on solvothermal synthesis and sonication. *Nat. Nanotechnol.* **2009**, *4*, 30–33. [[CrossRef](#)] [[PubMed](#)]
21. Rollings, E.; Gweon, G.-H.; Zhou, S.Y.; Mun, B.S.; McChesney, J.L.; Hussain, B.S.; Fedorov, A.V.; First, P.N.; de Heer, W.A.; Lanzara, A. Synthesis and characterization of atomically thin graphite films on a silicon carbide substrate. *J. Phys. Chem. Solids* **2006**, *67*, 2172–2177. [[CrossRef](#)]
22. Li, S.; Deng, D.; Shi, Q.; Liu, S. Electrochemical synthesis of a graphene sheet and gold nanoparticle-based nanocomposite, and its application to amperometric sensing of dopamine. *Microchim. Acta* **2012**, *177*, 325–331. [[CrossRef](#)]
23. Emtsev, K.V.; Bostwick, A.; Horn, K.; Jobst, J.; Kellogg, G.L.; Ley, L.; McChesney, J.L.; Ohta, T.; Reshanov, S.A.; Röhl, J.; *et al.* Towards wafer-size graphene layers by atmospheric pressure graphitization of silicon carbide. *Nat. Mater.* **2009**, *8*, 203–207. [[CrossRef](#)] [[PubMed](#)]
24. Sun, J.; Lindvall, N.; Cole, T.M.; Angel, K.T.T.; Teng, W.; Teo, K.B.K.; Chua, D.H.C.; Johan, L.; Yurgens, A. Low partial pressure chemical vapor deposition of graphene on copper. *IEEE Trans. Nanotechnol.* **2012**, *11*, 255–260. [[CrossRef](#)]
25. Batzill, M. The surface science of graphene: Metal interfaces, CVD synthesis, nanoribbons, chemical modifications, and defects. *Surf. Sci. Rep.* **2012**, *67*, 83–115. [[CrossRef](#)]
26. Hummers, S.; Offeman, R.E. Preparation of graphitic oxide. *J. Am. Chem. Soc.* **1958**, *80*, 1339. [[CrossRef](#)]
27. Lian, P.; Wang, J.; Cai, D.; Ding, L.; Jia, Q.; Wang, H. Porous SnO₂@C/graphene nanocomposite with 3D carbon conductive network as a superior anode material for lithium-ion batteries. *Electrochim. Acta* **2014**, *116*, 103–110. [[CrossRef](#)]

28. Liu, Y.-Z.; Li, Y.-F.; Yang, Y.-G.; Wen, Y.-F.; Wang, M.-Z. A one-pot method for producing ZnO-graphene nanocomposites from graphene oxide for supercapacitors. *Scr. Mater.* **2013**, *68*, 301–304. [[CrossRef](#)]
29. Dong, L.; Li, M.; Dong, L.; Zhao, M.; Feng, J.; Han, Y.; Deng, J.; Li, X.; Li, D.; Sun, X. Hydrothermal synthesis of mixed crystal phases TiO₂-reduced graphene oxide nanocomposites with small particle size for lithium ion batteries. *Int. J. Hydrog. Energ.* **2014**, *39*, 16116–16122. [[CrossRef](#)]
30. Yang, X.; Ding, H.; Zhang, D.; Yan, X.; Lu, C.; Qin, J.; Zhang, R.; Tang, H.; Song, H. Hydrothermal synthesis of MoO₃ nanobelt-graphene composites. *Cryst. Res. Technol.* **2011**, *46*, 1195–1201. [[CrossRef](#)]
31. Rabieh, S.; Nassimi, K.; Bagheri, M. Synthesis of hierarchical ZnO-reduced graphene oxide nanocomposites with enhanced adsorption-photocatalytic performance. *Mater. Lett.* **2016**, *162*, 28–31. [[CrossRef](#)]
32. Dai, J.; Song, M.; Wang, M.; Li, P.; Zhang, C.; Shen, Y.; Xie, A. Freeze-drying growth of Co₃O₄/N-doped reduced graphene oxide nanocomposite as excellent anode material for lithium-ion batteries. *Ceram. Int.* **2016**, *42*, 2410–2415. [[CrossRef](#)]
33. Nguyen-Phan, T.-D.; Pham, V.H.; Shin, E.W.; Pham, H.-D.; Kim, S.; Chung, J.S.; Kim, E.J.; Hur, S.H. The role of graphene oxide content on the adsorption-enhanced photocatalysis of titanium dioxide/graphene oxide composites. *Chem. Eng. J.* **2011**, *170*, 226–232. [[CrossRef](#)]
34. Nethravathi, C.; Viswanath, B.; Shivakumara, C.; Mahadevaiah, N.; Rajamathi, M. The production of smectite clay/graphene composites through delamination and co-stacking. *Carbon* **2008**, *46*, 1773–1781. [[CrossRef](#)]
35. Nethravathi, C.; Rajamathi, J.T.; Ravishankar, N.; Shivakumara, C.; Rajamathi, M. Graphite oxide-intercalated anionic clay and its decomposition to graphene-inorganic material nanocomposites. *Langmuir* **2008**, *24*, 8240–8244. [[CrossRef](#)] [[PubMed](#)]
36. Wu, J.; Shen, X.; Jiang, L.; Wang, K.; Chen, K. Solvothermal synthesis and characterization of sandwich-like graphene/ZnO nanocomposites. *Appl. Surf. Sci.* **2010**, *256*, 2826–2830. [[CrossRef](#)]
37. Chu, Y.H.; Yamagishi, M.; Wang, Z.M.; Kanoh, H.; Hirotsu, T. Synthesis of nanoporous graphite-derived carbon/TiO₂-SiO₂ composites by a mechanochemical intercalation method. *Micropor. Mesopor. Mater.* **2009**, *118*, 496–502. [[CrossRef](#)]
38. Wang, D.; Kou, R.; Choi, D.; Yang, Z.; Nie, Z.; Li, J.; Saraf, L.V.; Hu, D.; Zhang, J.; Graff, G.L.; *et al.* Ternary self-assembly of ordered metal oxide-graphene nanocomposites for electrochemical energy storage. *ACS Nano* **2010**, *4*, 1587–1595. [[CrossRef](#)] [[PubMed](#)]
39. Jiang, G.; Lin, Z.; Chen, C.; Zhu, L.; Chang, Q.; Wang, N.; Wei, W.; Tang, H. TiO₂ nanoparticles assembled on graphene oxide nanosheets with high photocatalytic activity for removal of pollutants. *Carbon* **2011**, *49*, 2693–2701. [[CrossRef](#)]
40. Liang, Y.T.; Vijayan, B.K.; Gray, K.A.; Hersam, M.C. Minimizing graphene defects enhances titania nanocomposite-based photocatalytic reduction of CO₂ for improved solar fuel production. *Nano Lett.* **2011**, *11*, 2865–2870. [[CrossRef](#)] [[PubMed](#)]
41. Stengl, V.; Popelkova, D.; Vlacil, P. TiO₂-graphene nanocomposite as high performance photocatalysts. *J. Phys. Chem. C.* **2011**, *115*, 25209–25218. [[CrossRef](#)]
42. Nurzulaikha, R.; Lim, H.N.; Harrison, I.; Lim, S.S.; Pandikumar, A.; Huang, N.M.; Lim, S.P.; Thien, G.S.H.; Yusoff, N.; Ibrahim, I. Graphene/SnO₂ nanocomposite-modified electrode for electrochemical detection of dopamine. *Sens. Biosens. Res.* **2015**, *5*, 42–49. [[CrossRef](#)]
43. Dutta, D.; Hazra, S.K.; Das, J.; Sarkar, C.; Basu, S. Studies on p-TiO₂/n-graphene heterojunction for hydrogen detection. *Sens. Actuators B* **2015**, *212*, 84–92. [[CrossRef](#)]
44. Burkhanov, G.S.; Gorina, N.B.; Kolchugina, N.B.; Roshan, N.R.; Slovetsky, D.I.; Chistov, E.M. Palladium-based alloy membranes for separation of high purity hydrogen from hydrogen-containing gas mixtures. *Platin. Metals Rev.* **2011**, *55*, 3–12. [[CrossRef](#)]
45. Singh, N.B.; Bhattacharya, B.; Sarkar, U. Nickel decorated single-wall carbon nanotube as CO sensor. *Soft Nanosci. Lett.* **2013**, *3*, 9–11. [[CrossRef](#)]
46. Wang, X.; Tabakman, S.M.; Dai, H. Atomic layer deposition of metal oxides on pristine and functionalized graphene. *J. Am. Chem. Soc.* **2008**, *130*, 8152–8153. [[CrossRef](#)] [[PubMed](#)]
47. Zhang, R.; Alecrim, V.; Andres, M.H.B.; Forsberg, S.; Andersson, M.; Olin, H. Thermally reduced kaolin-graphene oxide nanocomposites for gas sensing. *Sci. Rep.* **2015**, *5*. [[CrossRef](#)] [[PubMed](#)]
48. Srivastava, S.; Jain, K.; Singh, V.N.; Singh, S.; Vijayan, N.; Dilawar, N.; Gupta, G.; Senguttuvan, T.D. Faster response of NO₂ sensing in graphene-WO₃ nanocomposites. *Nanotechnology* **2012**, *23*. [[CrossRef](#)] [[PubMed](#)]

49. Lu, G.; Ocola, L.E.; Chen, J. Gas detection using low-temperature reduced graphene oxide sheets. *Appl. Phys. Lett.* **2009**, *94*, 083111. [[CrossRef](#)]
50. Esfandiari, A.; Irajizad, A.; Akhavan, O.; Ghasemi, S.; Gholami, M.R. Pd-WO₃/reduced graphene oxide hierarchical nanostructures as efficient hydrogen gas sensors. *Int. J. Hydrog. Energy* **2014**, *39*, 8169–8179. [[CrossRef](#)]
51. Breyse, M.; Claudel, B.; Faure, L.; Wolkenstein, T. Chemiluminescence during the catalysis of carbon monoxide oxidation on a thoria surface. *J. Catal.* **1976**, *45*, 137–144. [[CrossRef](#)]
52. Song, H.; Zhang, L.; He, C.; Qu, Y.; Tiana, Y.; Lv, Y. Graphene sheets decorated with SnO₂ nanoparticles: *In situ* synthesis and highly efficient materials for cataluminescence gas sensors. *J. Mater. Chem.* **2011**, *21*, 5972–5977. [[CrossRef](#)]
53. Zhang, D.; Liu, A.; Chang, H.; Xia, B. Room-temperature high-performance acetone gas sensor based on hydrothermal synthesized SnO₂-reduced graphene oxide hybrid composite. *RSC Adv.* **2015**, *5*, 3016–3022. [[CrossRef](#)]
54. Lin, Q.; Li, Y.; Yang, M. Tin oxide/graphene composite fabricated via a hydrothermal method for gas sensors working at room temperature. *Sens. Actuators B Chem.* **2012**, *173*, 139–147. [[CrossRef](#)]
55. Mishra, R.K.; Upadhyay, S.B.; Kushwaha, A.; Kim, T.-H.; Murali, G.; Verma, R.; Srivastava, M.; Singh, J.; Sahay, P.P.; Hee Lee, S. SnO₂ quantum dots decorated on RGO: A superior sensitive, selective and reproducible performance for a H₂ and LPG sensor. *Nanoscale* **2015**, *7*, 11971–11979. [[CrossRef](#)] [[PubMed](#)]
56. Nemade, K.R.; Waghuley, S.A. LPG sensing by graphene/ZnO quantum dots composite. *Int. J. ChemTech Res.* **2014**, *6*, 3399–3401.
57. Anand, K.; Singh, O.; Singh, M.P.; Kaur, J.; Singh, R.C. Hydrogen sensor based on graphene/ZnO nanocomposite. *Sens. Actuators B* **2014**, *195*, 409–415. [[CrossRef](#)]
58. Iftekhar Uddin, A.S.M.; Phan, D.-T.; Chung, G.-S. Low temperature acetylene gas sensor based on Ag nanoparticles-loaded ZnO-reduced graphene oxide hybrid. *Sens. Actuators B* **2015**, *207*, 362–369. [[CrossRef](#)]
59. Mu, H.; Zhang, Z.; Zhao, X.; Liu, F.; Wang, K.; Xie, H. High sensitive formaldehyde graphene gas sensor modified by atomic layer deposition zinc oxide films. *Appl. Phys. Lett.* **2014**, *105*. [[CrossRef](#)]
60. Jebreil Khadem, S.M.; Abdi, Y.; Darbari, S.; Ostovari, F. Investigating the effect of gas absorption on the electromechanical and electrochemical behavior of graphene/ZnO structure, suitable for highly selective and sensitive gas sensors. *Curr. Appl. Phys.* **2014**, *14*, 1498–1503. [[CrossRef](#)]
61. Zhong, L.; Yun, K. Graphene oxide-modified ZnO particles: Synthesis, characterization, and antibacterial properties. *Int. J. Nanomed.* **2015**, *10*, 79–92.
62. Kumar, N.; Srivastava, A.K.; Patel, H.S.; Gupta, B.K.; Varma, G.D. Facile synthesis of ZnO-reduced graphene oxide nanocomposites for NO₂ gas sensing applications. *Eur. J. Inorg. Chem.* **2015**, *2015*, 1912–1923. [[CrossRef](#)]
63. How, G.T.S.; Pandikumar, A.; Ming, H.N.; Ngee, L.H. Highly exposed {001} facets of titanium dioxide modified with reduced graphene oxide for dopamine sensing. *Sci. Rep.* **2014**, *4*, 5044. [[CrossRef](#)] [[PubMed](#)]
64. Fan, Y.; Lu, H.-T.; Liu, J.-H.; Yang, C.-P.; Jing, Q.-S.; Zhang, Y.-X.; Yang, X.-K.; Huang, K.-J. Hydrothermal preparation and electrochemical sensing properties of TiO₂-graphene nanocomposite. *Colloids Surf. B* **2011**, *83*, 78–82. [[CrossRef](#)] [[PubMed](#)]
65. Xu, C.-X.; Huang, K.-J.; Fan, Y.; Wu, Z.-W.; Li, J.; Gan, T. Simultaneous electrochemical determination of dopamine and tryptophan using a TiO₂-graphene/poly(4-aminobenzenesulfonic acid) composite film based platform. *Mater. Sci. Eng. C* **2012**, *32*, 969–974.
66. Jang, H.D.; Kim, S.K.; Chang, H.C.; Jo, E.H.; Roh, K.M.; Choi, J.-H.; Choi, J.-W. Synthesis of 3D silver-graphene-titanium dioxide composite via aerosol spray pyrolysis for sensitive glucose biosensor. *Aerosol Sci. Tech.* **2015**, *49*, 538–546. [[CrossRef](#)]
67. Chang, B.Y.S.; Huang, N.M.; An'amt, M.N.; Marlinda, A.R.; Norazriena, Y.; Muhamad, M.R.; Harrison, I.; Lim, H.N.; Chia, C.H. Facile hydrothermal preparation of titanium dioxide decorated reduced graphene oxide nanocomposite. *Int. J. Nanomed.* **2012**, *7*, 3379–3387.
68. Wang, T.; Peng, Z.; Wang, Y.; Tang, J.; Zheng, G. MnO nanoparticle@mesoporous carbon composites grown on conducting substrates featuring high-performance lithium-ion battery, supercapacitor and sensor. *Sci. Rep.* **2013**. [[CrossRef](#)] [[PubMed](#)]

69. Xiang, C.; Jiang, D.; Zou, Y.; Chu, H.; Qiu, S.; Zhang, H.; Xu, F.; Sun, L.; Zheng, L. Ammonia sensor based on polypyrrole-graphene nanocomposite decorated with titania nanoparticles. *Ceram. Int.* **2015**, *41*, 6432–6438. [[CrossRef](#)]
70. Liu, S.; Wang, Z.; Zhang, Y.; Zhang, C.; Zhang, T. High performance room temperature NO₂ sensors based on reduced graphene oxide-multiwalled carbon nanotubes-tin oxide nanoparticles hybrids. *Sens. Actuators B* **2015**, *211*, 318–324. [[CrossRef](#)]
71. Liu, S.; Zhou, L.; Yao, L.; Chai, L.; Li, L.; Zhang, G.; Kankan; Shi, K. One-pot reflux method synthesis of cobalt hydroxide nanoflake-reduced graphene oxide hybrid and their NO_x gas sensors at room temperature. *J. Alloys Compd.* **2014**, *612*, 126–133. [[CrossRef](#)]
72. Zhang, H.; Feng, J.; Fei, T.; Liu, S.; Zhang, T. SnO₂ nanoparticles-reduced graphene oxide nanocomposites for NO₂ sensing at low operating temperature. *Sens. Actuators B* **2014**, *190*, 472–478. [[CrossRef](#)]
73. Li, L.; He, S.; Liu, M.; Zhang, C.; Chen, W. Three-dimensional mesoporous graphene aerogel-supported SnO₂ nanocrystals for high-performance NO₂ gas sensing at low temperature. *Anal. Chem.* **2015**, *87*, 1638–1645. [[CrossRef](#)] [[PubMed](#)]
74. Jiang, Z.; Li, J.; Aslan, H.; Li, Q.; Li, Y.; Chen, M.; Huang, Y.; Froning, J.P.; Otyepka, M.; Zboril, R.; Besenbacher, F.; Dong, M. A high efficiency H₂S gas sensor material: Paper like Fe₂O₃/graphene nanosheets and structural alignment dependency of device efficiency. *J. Mater. Chem. A* **2014**, *2*, 6714–6717. [[CrossRef](#)]
75. MalekAlaie, M.; Jahangiri, M.; Rashidi, A.M.; HaghighiAsl, A.; Izadi, N. Selective hydrogen sulfide (H₂S) sensors based on molybdenum trioxide (MoO₃) nanoparticle decorated reduced graphene oxide. *Mater. Sci. Semicond. Process.* **2015**, *38*, 93–100. [[CrossRef](#)]
76. Latif, U.; Dickert, F.L. Graphene hybrid materials in gas sensing applications. *Sensors* **2015**, *15*, 30504–30524. [[CrossRef](#)] [[PubMed](#)]
77. Han, X.; Li, S.; Peng, Z.; Al-Yuobi, A.O.; Omar Bashammakh, A.S.; El-Shahawi, M.S.; Leblanc, R.M. Interactions between carbon nanomaterials and biomolecules. *J. Oleo Sci.* **2016**, *65*. [[CrossRef](#)] [[PubMed](#)]



© 2016 by the authors; licensee MDPI, Basel, Switzerland. This article is an open access article distributed under the terms and conditions of the Creative Commons Attribution (CC-BY) license (<http://creativecommons.org/licenses/by/4.0/>).